Kovove Mater. 49 2011 29–36
DOI: 10.4149/km_2011_1_29

The effect of deformation processing on tensile ductility of magnesium alloy AZ31

Z. Zuberova[1]*, I. Sabirov[2], Y. Estrin[3,4]

[1] *Bosch Rexroth AG, An den Kelterwiesen 14, 72160 Horb am Neckar, Germany*
[2] *Instituto Madrileño de Estudios Avanzados de Materiales, IMDEA Materials Institute, E.T.S. de Ingenieros de Caminos, 28040, Madrid, Spain*
[3] *ARC Centre of Excellence for Design in Light Alloys, Department of Materials Engineering, Monash University, Clayton, 3800 VIC, Australia*
[4] *CSIRO Division of Process Science and Engineering, Clayton South, 3169 VIC, Australia*

Received 13 April 2010, received in revised form 30 August 2010, accepted 31 August 2010

Abstract

A cast magnesium alloy AZ31 was subjected to two different thermo-mechanical process routes, *viz.* hot cross rolling and hot cross rolling with subsequent equal channel angular pressing. The effect of the deformation processing on the tensile behaviour of the alloy was investigated and interpreted in terms of microstructure and texture effects. In particular, the tensile ductility and its relation to the strain hardening rate and the instantaneous strain rate sensitivity were studied. It was demonstrated that Hart's necking criterion provides an excellent vehicle for assessment of tensile ductility of the alloy.

K e y w o r d s: magnesium alloy, hot cross rolling, equal channel angular pressing, mechanical properties, strain rate sensitivity

1. Introduction

Reduction of the grain size of a polycrystalline metallic material commonly has a beneficial effect on its mechanical properties. Strength usually increases upon grain refinement according to the well-known Hall-Petch relation [1, 2]; the uniform elongation may improve as well. However, when the microstructure is refined down to the sub-micron scale, the uniform elongation drops dramatically, falling victim to strain localization and premature failure [3–5].

Ductility is very important for many shaping and forming operations and also for avoiding catastrophic failure in load-bearing parts. Several strategies were developed to increase the uniform elongation of ultra-fine grained metallic materials [6]. One of these strategies is based on the utilization of increased strain rate sensitivity (SRS) of the flow stress, which enters the Hart condition [7] for the onset of tensile necking:

$$\theta/\sigma + m = 1. \qquad (1)$$

Here σ is the flow stress and θ is its derivative with respect to plastic strain ε, i.e. the strain hardening coefficient. The parameter m is the strain rate sensitivity index defined below. The familiar Considère criterion for neck initiation follows from Eq. (1) if the strain rate sensitivity is low and m can be neglected.

Equation (1) shows that the resistance of a material to strain localization can be increased either by raising its strain hardening capability or the strain rate sensitivity of stress, or both. Grain refinement down to the sub-micron range generally leads to an increase of the SRS owing to a greater contribution of diffusion controlled processes to plastic deformation and – unfortunately – to a concurrent loss of strain hardening [8]. Which one of the two contributing terms is affected by grain refinement more cannot be determined *a priori*, and detailed measurements are required to assess their relative contributions.

The strain rate sensitivity of the flow stress is especially important for Mg alloys, which suffer from low ductility at room temperature. The mechanical beha-

*Corresponding author: tel.: +49 745 1921908; fax: +49 711 8115139135; e-mail address: Zuzana.Zuberova@boschrexroth.de

Table 1. Chemical composition (wt.%) of the AZ31 alloy

Mg	Al	Mn	Zn	Ca	Si	Pb	Sn	Zr
94.500	3.623	0.292	1.361	> 0.180	0.0145	0.0137	< 0.0200	< 0.0100

viour of the broadly used structural alloy AZ31 shows strong strain rate dependence at room temperature [9]. Hot rolling with subsequent annealing [10, 11] as well as various methods of severe plastic deformation [12–14] have been used for grain refinement in the alloy in the past. The aim of the present work was to get a better insight in the effect of the microstructure produced by hot cross rolling and equal channel angular pressing (ECAP) on the strain hardening and the strain rate sensitivity of stress – and ultimately on the room temperature tensile ductility of AZ31.

2. Materials

The chemical composition of the AZ31 alloy used in this study is given in Table 1. Three different conditions of the material, corresponding to three different processing histories, were investigated:

1. *Squeeze casting.* Squeeze casting was performed at ZfW GmbH (Clausthal-Zellerfeld, Germany) in a two-step loading process (pressure of 80 MPa for 15 s and then pressure of 140 MPa for 90 s). The temperature of the melt was 720 ℃ and the die temperature was 200 ℃. Casting was done under a protective gas atmosphere of Ar-SF_6. Henceforth, this condition will be referred to as SC.

2. *Hot cross rolling.* Hot cross rolling of the alloy was performed at MgF GmbH (Freiberg, Germany). As-cast material was subjected to hot rolling at 370 ℃ with a total reduction ratio of 85 %. The maximum reduction ratio in a single pass was 10 %. Between passes the plate was rotated by 90°, always in the same sense. Below, this condition will be referred to as HR.

3. *Equal channel angular pressing (ECAP).* Billets with dimensions of 10 mm × 10 mm × 100 mm were machined from HR AZ31. The longitudinal axis of a billet was parallel to the direction of the last rolling pass. The billets were subjected to four ECAP passes at 200 ℃. Route B_c, which involves rotation of the billet by 90° about its axis between the passes, was employed. The ECAP die had an intersection angle of $\Phi = 90°$ between the two channels and a zero arc curvature angle. The ram speed was 5 mm min^{-1}. A heat resistant MoS_2 lubricant was used to reduce friction between the sample and the die.

3. Experimental procedures

The microstructure was analysed using a ZEISS Axioplan light microscope. Samples were mechanically polished using silica colloidal solution at the final stage. The samples were etched using a solution consisting of 100 ml H_2O, 100 ml ethanol, and 5 g picric acid. The average grain size was determined using the linear intercept method. At least three hundred grains were measured to obtain the average grain size.

To study the microstructure at a finer scale, transmission electron microscopy (TEM) was carried out using a Philips CM20 microscope operating at 200 kV. Foils for TEM study were prepared by twin jet electropolishing with a LiCl + magnesium perchlorate + methanol + buthyloxyethanol solution at ∼ 45 ℃. Observations were made in both the bright and the dark field imaging modes, and selected area electron diffraction (SAED) patterns were recorded from the areas of interest.

The global texture of AZ31 in the three conditions was investigated using the TEX-2 four-circle diffractometer of the neutron diffraction system at GKSS Geesthacht, Germany, cf. for detail of the experimental facility [15].

Most of the results relating to the microstructure and texture of the material in the three conditions have been reported in earlier publications [13, 15, 16], so that the focus in this communication will be on the tensile ductility results, which have not been published before.

Cylindrical tensile samples with a gauge length of 25 mm and a diameter of 5 mm were machined from SC and HR material. The tensile axis of HR samples was parallel to the rolling direction of the last rolling pass. Due to limitations on the length and cross-sectional dimensions of the ECAP-processed billets, cylindrical samples with a smaller gauge length (20 mm) and a smaller diameter (4 mm) were used for subsequent tensile testing. The tensile axis of the ECAP processed samples was parallel to the pressing direction. Tensile tests with a constant cross-head speed were carried out using a 100 kN INSTRON universal testing machine with a 5 kN load cell. The cross-head speed corresponded to the initial strain rate of $10^{-3}\,s^{-1}$. The strain hardening rate was determined by differentiation of the monotonic tensile curves using piece-wise polynomial fitting through 5 or 10 data points on the stress-strain curve in a sliding manner.

To estimate the strain rate sensitivity index, m, strain rate jump tests were performed at the base strain rate of $10^{-4}\,s^{-1}$. Jumps in the strain rate ($10^{-4}\,s^{-1} \rightarrow 10^{-3}\,s^{-1} \rightarrow 10^{-4}\,s^{-1}$) were imposed repetitively, starting from a strain of 1 % and then go-

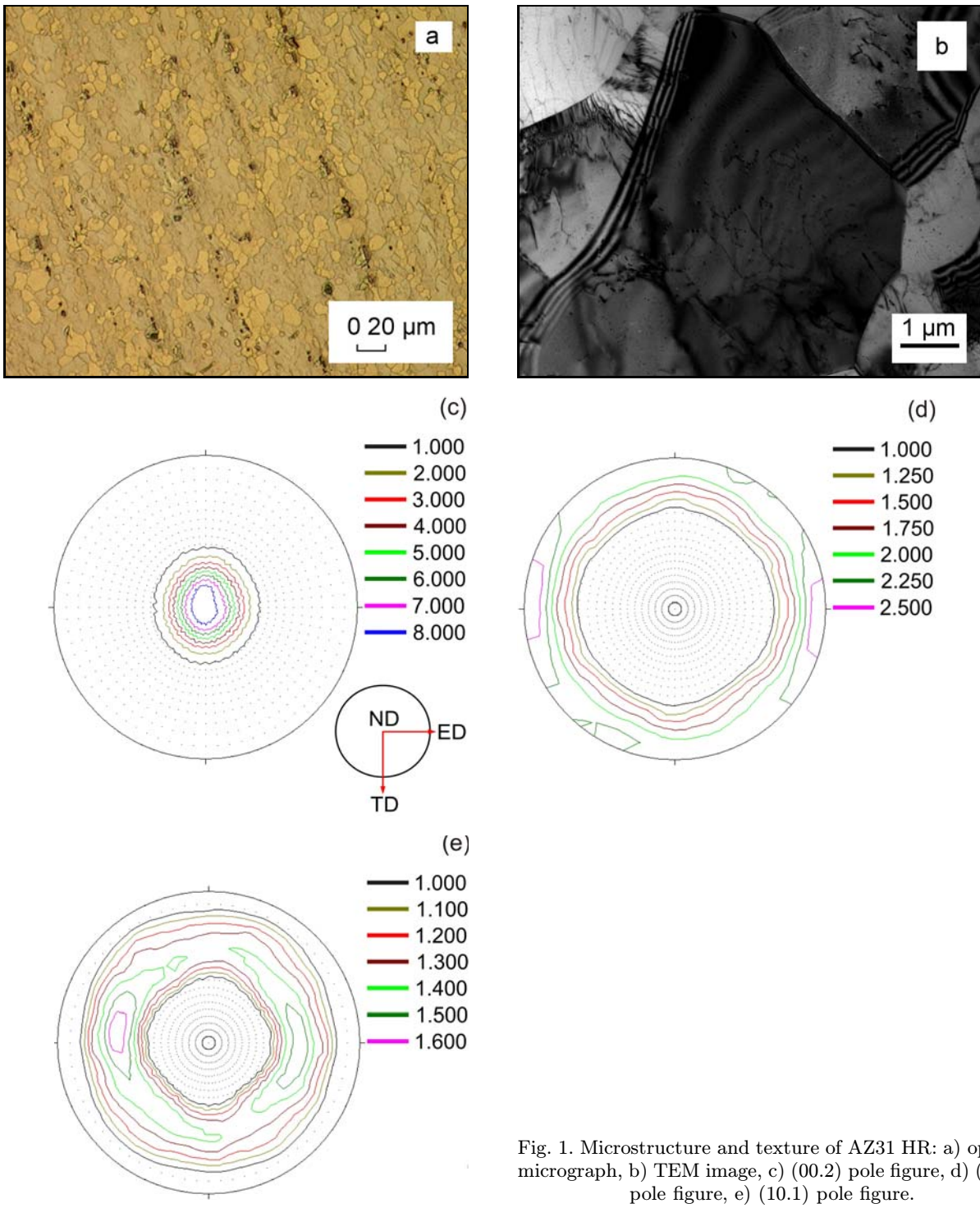

Fig. 1. Microstructure and texture of AZ31 HR: a) optical micrograph, b) TEM image, c) (00.2) pole figure, d) (10.0) pole figure, e) (10.1) pole figure.

ing in steps of 1 % until failure of the specimen. The strain between the strain rate jumps was sufficient for possible transient effects associated with the inertia of the testing machine to die off. The m-values were calculated using the following standard equation until failure of the specimen [7, 8, 17]:

$$m = \frac{\partial \ln \sigma}{\partial \ln \dot{\varepsilon}} = \frac{\ln(\sigma_2/\sigma_1)}{\ln(\dot{\varepsilon}_2/\dot{\varepsilon}_1)}, \qquad (2)$$

where σ_2 and σ_1 are the values of the flow stress corresponding to the strain rates of $\dot{\varepsilon}_2$ and $\dot{\varepsilon}_1$, respectively, taken immediately after and just before a strain rate jump. Back-extrapolation of the stress--strain curve to the strain at which the strain rate jump was made was used to determine the σ_2 values and the SRS index m, which in light of the procedure used to determine it is referred to as the *instantaneous* strain rate sensitivity index [17].

Table 2. Average grain size, mechanical properties under tensile deformation and tensile elongation at necking predicted for AZ31 on the basis of the Hart criterion

AZ 31	Grain size (μm)	Yield stress (MPa)	Ultimate tensile strength (MPa)	Uniform elongation (%)	ε_u^{Hart} (%)
SC	250	86	187	9.1	9.1
HR	15	214	328	17.5	14.5
ECAP	2.5	164	319	24.0	23.8

4. Results

4.1. Microstructure of the AZ31 alloy in different conditions

The microstructure of the SC alloy had a pronounced dendritic appearance [16]. The microstructure was homogeneous throughout a metallographic specimen. No twins were observed in optical micrographs. The grain size varied in the range of 150 to 450 μm, with an average estimated at 250 μm [13, 16]. The SC alloy showed a random texture [16].

The HR specimens were cut from a rolled sheet with dimensions of 320 mm × 470 mm × 18 mm. For microstructural investigations longitudinal and normal sections were made. The microstructure of the HR material shown in Fig. 1a [13, 16] is homogeneous and consists of nearly equiaxed grains with the average size of 15 μm. TEM study showed that the grain interior was dislocation-free (Fig. 1b [16]). Only a few dislocations can be seen at grain boundaries. An earlier study [16] showed that the HR material had a strong basal texture typical for hot rolled Mg alloys, cf. Fig. 1c–e. No evident preference for any crystallographic direction to align with the rolling direction was found in [16].

Optical microscopy and TEM investigations of the sections of the ECAP processed material normal to the pressing direction revealed a microstructure consisting of nearly equiaxed grains with the average size of 2.5 μm (Fig. 2a [13, 16]). No twins were observed. Most of the grains were devoid of dislocations, while presence of dislocations at some grain boundaries was noted (Fig. 2b [13, 16]). The grain boundaries had a characteristic contrast typical of equilibrium boundaries. The misorientation between individual grains as determined by electron diffraction confirmed the predominantly high angle ($> 15°$) character of grain boundaries. It should be noted that the ECAP processed material has a much more pronounced texture than in the HR or SC material, cf. Fig. 2c–f [16]. A similarly pronounced texture was found for pure magnesium processed by ECAP [14], where after ECAP the basal planes were predominantly inclined at $\sim 45°$ to the pressing direction (billet axis) – an observation made earlier by Mukai et al. [18] and Agnew et al. [19].

4.2. Deformation behaviour of the AZ31 alloy in different conditions

The monotonic tensile true stress-true strain curves for all conditions studied are presented in Fig. 3a. The mechanical properties of alloy AZ31 in the three different conditions under consideration are compared in Table 2. It is seen that the SC alloy exhibits the lowest tensile strength and ductility, whereas the HR material shows the highest tensile strength (328 MPa) and a large value of uniform elongation (17.5 %). ECAP material exhibits a slightly lower tensile strength, 319 MPa, but a higher uniform elongation (24 %) compared with the HR material. The diagrams showing the dependence of the strain hardening coefficient on the true stress for all conditions are shown in Fig. 3b. The overall range of stress variation in the plastic region is the largest for the ECAP material (Fig. 3a). The ECAP material also shows the largest capacity for strain hardening in terms of the difference between the ultimate tensile strength and the yields strength, $\sigma_{UTS} - \sigma_y$, which is about 155 MPa. The corresponding values for the HR material ($\sim$ 114 MPa) and the SC material ($\sim$ 100 MPa) are significantly lower. With its largest strain hardening ability, the ECAP material exhibits the highest tensile ductility among all three conditions tested.

Figure 4a illustrates characteristic response of the SC, HR, and ECAP materials to imposed strain rate jumps. The evolution of the parameter m during a tensile test for all conditions is presented in Fig. 4b. It is evident that in all three conditions the m-value decreases with increasing flow stress first and then picks up after reaching a minimum. The highest m-value was found for AZ31 ECAP ($m \sim 0.02$), whereas AZ31 SC showed the lowest values ($m \sim 0.003$–0.007). As expected, the m-values are higher for smaller grain size. The scatter in the m-values is insignificant for all three conditions studied, so the trend has been documented clearly.

Given the relatively high strain rate sensitivity observed, it is appropriate to employ the Hart criterion, Eq. (1), rather than the Considère criterion, to estimate theoretically the value of the uniform elongation

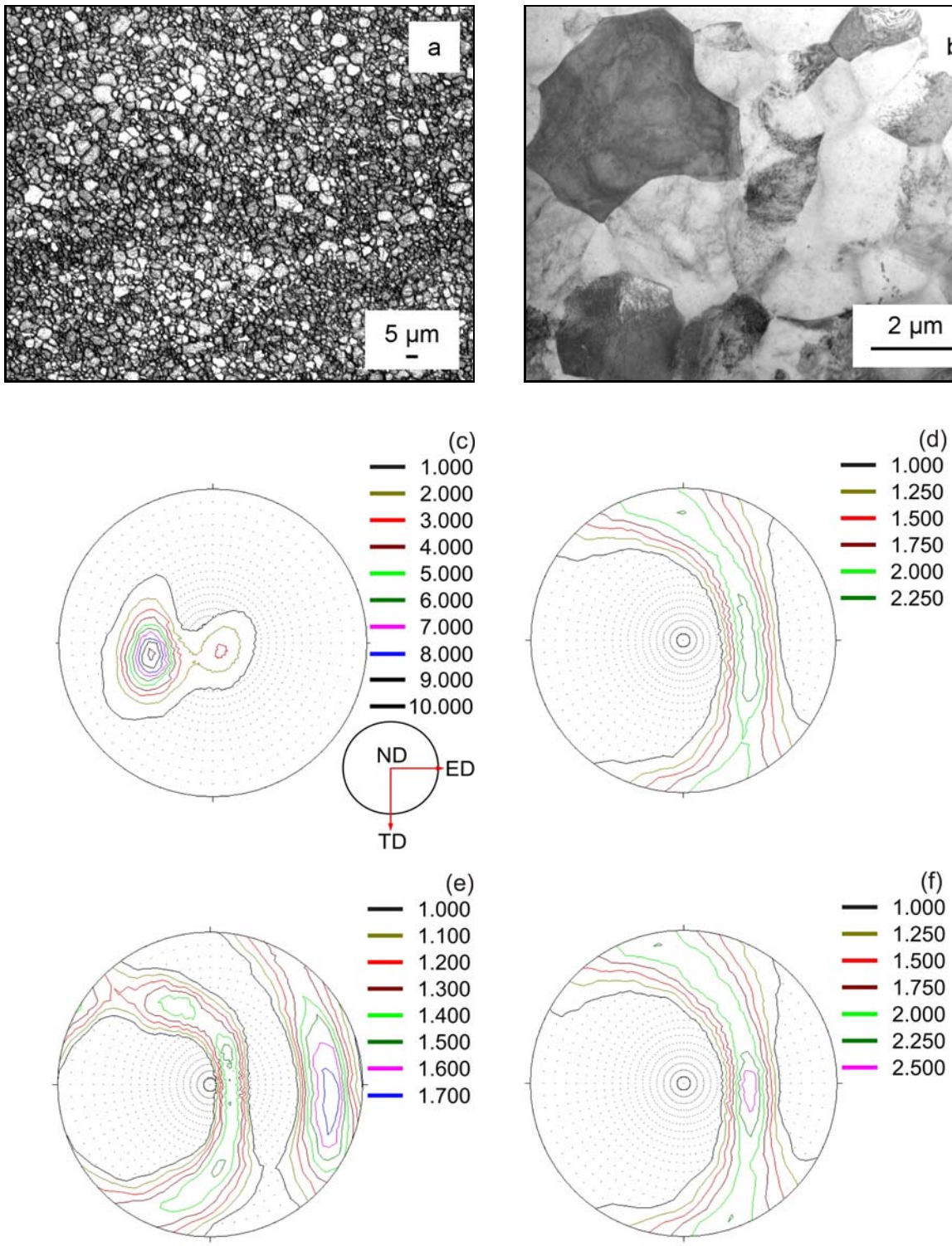

Fig. 2. Microstructure and texture of AZ31 ECAP: a) optical micrograph, b) TEM image, c) (00.2) pole figure, d) (10.0) pole figure, e) (10.1) pole figure, f) (11.0) pole figure.

for the materials studied. As seen from Table 2, the results of the theoretical prediction for the uniform elongation, ε_u^{Hart}, are in very good agreement with the experimental data.

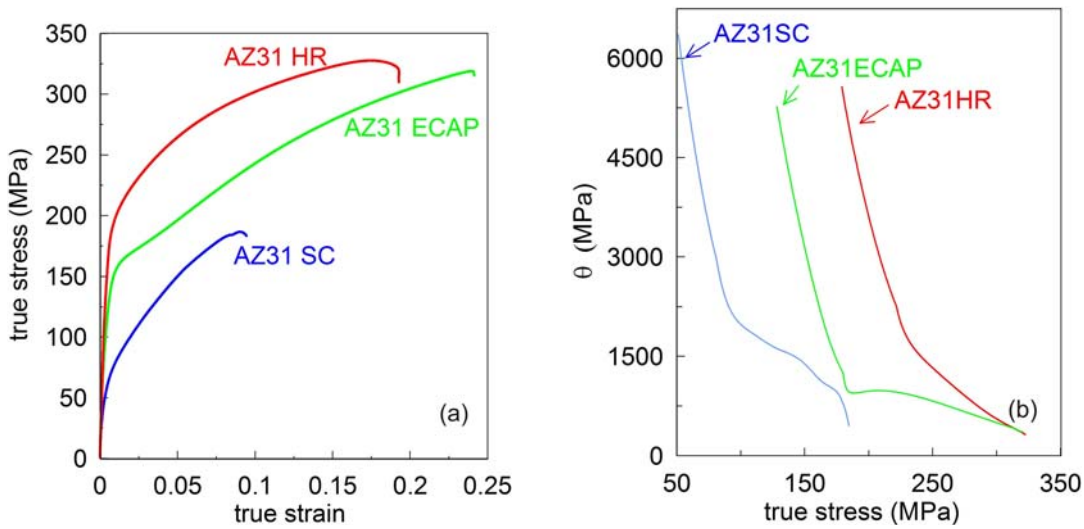

Fig. 3. Mechanical properties of the AZ31 alloy: a) true stress-true strain curves, b) strain hardening rate-true stress curves.

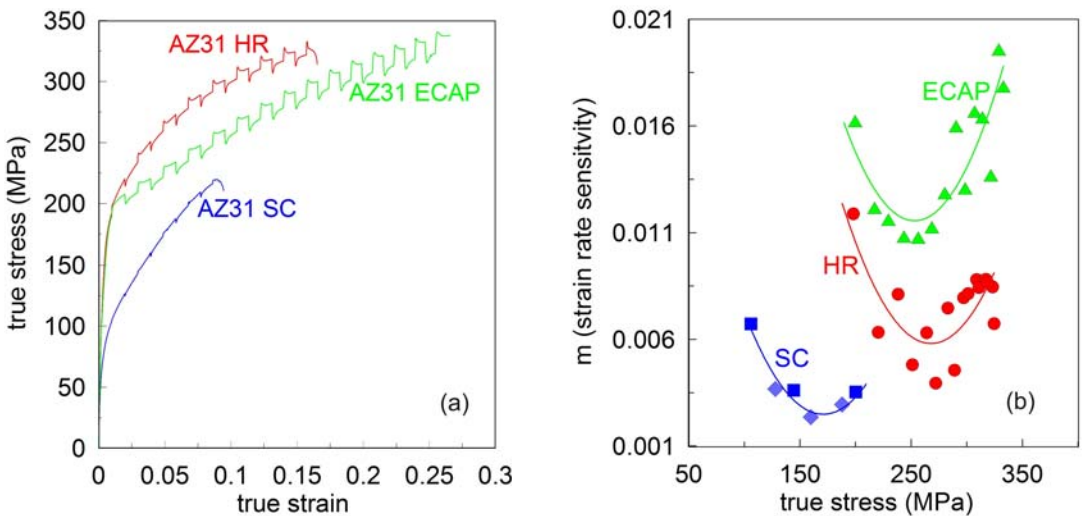

Fig. 4. Mechanical properties of AZ31 alloy: a) strain rate jump tests, b) strain rate sensitivity index vs. true stress curves.

5. Discussion

5.1. The effect of deformation processing on mechanical properties

The above results show that – through its effect on the grain structure and texture – the mechanical processing employed in this work affects the mechanical strength and tensile deformation behaviour of the material in a significant way. Coarse grained SC material with random texture possesses the lowest mechanical strength, but a high strain hardening rate (Fig. 3a). This may be explained in terms of random texture, which provides an activation of different mechanisms in different grains depending on their individual orientation with respect to the tensile axis. A combination of slip and twinning in grains where twins act as barriers to gliding dislocations thus effectively decreasing the grain size, results in a high rate of strain hardening.

In the HR material, a strengthening effect of grain refinement according to the Hall-Petch relation is augmented by a texture effect. Indeed, the basal texture, with the c-axis perpendicular to the tensile direction, is not favourable for slip on the basal plane and twinning at low stress levels. Accordingly, higher stresses are necessary to activate the onset of plastic deformation. Interaction of slip and twinning during plastic deformation contributes to strain hardening and results in values of θ, which are higher than for the other two conditions (Fig. 3b). Consequently, the stress-strain curve for the HR material lies above the curves for SC and ECAP conditions. While both the strain hardening coefficient and the stress are increased over the

SC levels by hot rolling, the ratio θ/σ turns out to be higher for the HR material, meaning that it should have a higher tensile ductility. This favourable effect is further enhanced by a higher strain rate sensitivity of the flow stress, see Fig. 4b. Higher SRS may stem from a contribution to plastic strain from diffusion-controlled processes and also be associated strain-rate dependent propensity for twinning in alloy AZ31 [20]. Overall, the HR material shows a higher strength and a better tensile elongation than the SC material.

An interesting result is that further refinement of the grain structure of the HR material down to the average grain size of 2.5 μm produced by ECAP did not lead to any strengthening of the material, as might have been expected according to the Hall-Petch relation. In fact, ECAP treatment led to a decrease in strength (Fig. 3a)! An obvious explanation is the ensuing change in texture, whose softening effect due to the orientation of the basal planes conducive for crystallographic slip [18, 19] turns out to outstrip the Hall-Petch strengthening. Improved tensile ductility over that of the HR material is consistent with this explanation.

The results of this investigation demonstrate a strong effect of deformation by cross hot rolling and ECAP on the strain hardening of the AZ31 alloy. In [21], it was emphasized that strain hardening of magnesium alloys was influenced by both texture and the grain size. Unfortunately, in the present work it was not possible to separate these effects, as both the texture and the grain size were varied as a result of the processing used.

5.2. The effect of deformation processing on the strain rate sensitivity

A significant body of literature on the effect of grain size on the strain rate sensitivity of the flow stress in Mg alloys suggests that the SRS index m increases upon grain refinement. In [11], it was demonstrated for AZ31 that m went up from 0.009 to 0.017 when the grain size was reduced from 55 μm to 2.6 μm. This effect was attributed to an increase in the contribution of grain boundary sliding to plastic strain. Similar results were reported for the AZ31B alloy in [12], where the strain rate sensitivity index at room temperature estimated from strain rate jump tests increased from 0.009 to 0.029 when the average grain size was reduced from 10 μm to 2 μm. Our present results confirm this trend (Fig. 3d). Deformation processing by ECAP is more effective than that by cross hot rolling in terms of grain refinement and enhancement of strain rate sensitivity, but it does not provide the highest mechanical strength (Fig. 3a). It has been suggested [22, 23] that diffusion controlled plastic flow within the grains and in the grain boundaries is responsible for enhanced strain rate sensitivity of the flow stress of ultrafine grained materials (with cubic structure in the cases reported in [22, 23]). This increase in strain rate sensitivity compensates for a loss in the strain hardening rate, which occurs upon ECAP processing of the HR material, and gives rise to higher uniform elongation (Table 2). The results of the present investigation show that theoretical prediction of uniform tensile elongation based on the Hart criterion, which accounts for both the strain hardening and the strain rate sensitivity effects, is in good agreement with experiment (Table 2).

Despite this more than satisfactory confirmation of the potency of the Hart criterion, one should be aware of the fact that the criterion is a mechanistic one. To control the processing steps targeting improved strength and ductility, a detailed understanding of the intricate interplay between their effects on microstructure and texture, and through that on the strain hardening and the strain rate sensitivity of stress, is required. Some insights in these effects have been provided in this communication, but more work is needed to 'de-convolute' the grain structure and the texture effects.

We also note that Hart criterion may fail as a predictive tool, particularly if deformation is non-uniform at meso- or macro-scale, as was the case with an ultrafine grained Al alloy tested at room temperature [24].

6. Conclusions

The effect of hot cross rolling at 370 ℃ and equal channel angular pressing at 200 ℃ on the microstructure of a cast magnesium alloy AZ31 was investigated. The grain size was reduced from 250 μm to 15 μm after hot cross rolling and to 2.5 μm after subsequent ECAP processing. The highest tensile strength (328 MPa) was achieved by hot cross rolling of the alloy. Further ECAP processing, while raising uniform tensile elongation of AZ31 to a level of 24 %, led to a drop in its mechanical strength. In keeping with the ideas presented in [17] and [18], this finding demonstrates that in the case of AZ31 considered, texture softening has a stronger effect on the flow stress than strengthening by grain refinement. The tensile ductility of ECAP processed material was promoted by increased strain rate sensitivity of flow stress in this material. An excellent predictive capability of the Hart necking criterion was demonstrated.

Acknowledgements

The authors acknowledge financial support from the Australian Research Council through the ARC Centre of Excellence for Design in Light Metals. One of the authors (YE) would like to acknowledge partial support from the

National Research Foundation of Korea through the World Class University Program at Seoul National University, funded by the Ministry of Education, Science and Technology (R31-2008-000-10075-0). IS thanks the FP7 Marie Curie Action – People for the AMAROUT Fellowship (COFUND programme). Texture measurements referred to in this publication were done by Dr. W. Gan. Valuable discussions with Prof. H.-G. Brokmeier and Dr. S. B. Yi are gratefully appreciated. The authors are also grateful to T. T. Lamark for his apt assistance with ECAP experiments. TEM micrographs in Figs. 1–3 were reproduced from Figs. 1–3 of [15] with kind permission from Springer Science + Business Media.

References

[1] HALL, E. O.: Proc. Phys. Soc. B, *64*, 1951, p. 747. doi:10.1088/0370-1301/64/9/303
[2] PETCH, N. J.: J. Iron Steel Inst., *174*, 1953, p. 25.
[3] VALIEV, R. Z.—ESTRIN, Y.—HORITA, Z.—LANGDON, T. G.—ZEHETBAUER, M. J.—ZHU, Y. T.: JOM, *58*, 2006, p. 33. doi:10.1007/s11837-006-0213-7
[4] WANG, Y. M.—MA, E.: Mater. Sci. Engng. A, *375–377*, 2004, p. 46. doi:10.1016/j.msea.2003.10.214
[5] VALIEV, R. Z.—ISLAMGALIEV, R. K.—ALEXANDROV, I. V.: Prog. Mater. Sci., *45*, 2000, p. 103. doi:10.1016/S0079-6425(99)00007-9
[6] MA, E.: JOM, *58*, 2006, p. 49. doi:10.1007/s11837-006-0215-5
[7] HART, E. W.: Acta Mater., *15*, 1967, p. 351. doi:10.1016/0001-6160(67)90211-8
[8] KIM, H. S.—ESTRIN, Y.: Appl. Phys. Lett., *79*, 2001, p. 4115. doi:10.1063/1.1426697
[9] AGNEW, S. R.—DUYGULU, O.: Int. J. Plast., *21*, 2005, p. 1161. doi:10.1016/j.ijplas.2004.05.018
[10] STANFORD, N.—BARNETT, M. R.: J. Alloys Comp., *466*, 2008, p. 182. doi:10.1016/j.jallcom.2007.11.082
[11] DEL VALLE, J. A.—RUANO, O. A.: Scripta Mater., *55*, 2006, p. 775. doi:10.1016/j.scriptamat.2006.07.013
[12] YANG, Q.—GHOSH, A. K.: Acta Mater., *54*, 2006, p. 5159. doi:10.1016/j.actamat.2006.06.043
[13] ZUBEROVÁ, Z.—ESTRIN, Y.—LAMARK, T. T.—JANEČEK, M.—HELLMIG, R. J.—KRIEGER, M.: J. Mater. Proc. Tech., *184*, 2007, p. 294. doi:10.1016/j.jmatprotec.2006.11.098
[14] LUKÁČ, P.—KOCICH, R.—GREGER, M.—PADALKA, O.—SZÁRAZ, Z.: Kovove Mater., *45*, 2007, p. 115.
[15] BROKMEIER, H. G.—GAN, W.—ZHENG, M.—ZUBEROVA, Z.—ESTRIN, Y.: Mater. Sci. Forum, *584–586*, 2008, p. 748. doi:10.4028/www.scientific.net/MSF.584-586.748
[16] ZUBEROVÁ, Z.—KUNZ, L.—LAMARK, T. T.—ESTRIN, Y.—JANEČEK, M.: Metall Mater Trans A, *38*, 2007, p. 1934. doi:10.1007/s11661-007-9109-6
[17] CAILLARD, D.—MARTIN, J. L.: Thermally Activated Mechanisms in Crystal Plasticity. Oxford, Pergamon Materials Series, Elsevier 2003.
[18] MUKAI, T.—YAMANOI, M.—WATANABE, H.—HIGASHI, K.: Scripta Mater., *45*, 2001, p. 89. doi:10.1016/S1359-6462(01)00996-4
[19] AGNEW, R.—MEHRORTA, P.—LILLO, T. M.—STOICA, G. M.—LIAW, P. K.: Acta Mater., *53*, 2005, p. 3135. doi:10.1016/j.actamat.2005.02.019
[20] DAVIES, C. H. J.: Mater. Sci. Forum, *539–543*, 2007, p. 1723. doi:10.4028/www.scientific.net/MSF.539-543.1723
[21] DEL VALLE, J. A.—CARRENO, F.—RUANO, O. A.: Acta Mater., *54*, 2006, p. 4247. doi:10.1016/j.actamat.2006.05.018
[22] SABIROV, I.—BARNETT, M. R.—ESTRIN, Y.—HODGSON, P. D.: Scripta Mater., *61*, 2009, p. 181. doi:10.1016/j.scriptamat.2009.03.032
[23] MAY, J.—HOEPPEL, H. W.—GOKEN, M.: Mater. Sci. Forum, *503–504*, 2006, p. 781. doi:10.4028/www.scientific.net/MSF.503-504.781
[24] SABIROV, I.—ESTRIN, Y.—BARNETT, M. R.—TIMOKHINA, I.—HODGSON, P. D.: Scripta Mater., *58*, 2008, p. 163. doi:10.1016/j.scriptamat.2007.09.057